ORIGINAL ARTICLE

WILEY

Role of gut microbiome in the outcome of lymphoma patients treated with checkpoint inhibitors—The MicroLinf Study

Beatrice Casadei[1] | Gabriele Conti[2,3] | Monica Barone[2] | Silvia Turroni[3] | Serafina Guadagnuolo[1] | Alessandro Broccoli[1,4] | Patrizia Brigidi[2] | Lisa Argnani[4] | Pier Luigi Zinzani[1,4]

[1]Istituto di Ematologia "Seràgnoli", IRCCS Azienda Ospedaliero-Universitaria di Bologna, Bologna, Italy

[2]Human Microbiomics Unit, Department of Medical and Surgical Sciences, University of Bologna, Bologna, Italy

[3]Unit of Microbiome Science and Biotechnology, Department of Pharmacy and Biotechnology, University of Bologna, Bologna, Italy

[4]Dipartimento di Scienze Mediche e Chirurgiche, Università di Bologna, Bologna, Italy

Correspondence
Pier Luigi Zinzani, Dipartimento di Scienze Mediche e Chirurgiche, Università di Bologna, Via Massarenti, 9, Bologna 40138, Italy; Istituto di Ematologia "Seràgnoli", IRCCS Azienda Ospedaliero-Universitaria di Bologna, Via Massarenti, 9, Bologna 40138, Italy.
Email: pierluigi.zinzani@unibo.it

Funding information
Ministero della Salute

Abstract

Biomarkers for immune checkpoint inhibitors (ICIs) response and resistance include PD-L1 expression and other environmental factors, among which the gut microbiome (GM) is gaining increasing interest especially in lymphomas. To explore the potential role of GM in this clinical issue, feces of 30 relapsed/refractory lymphoma (Hodgkin and primary mediastinal B-cell lymphoma) patients undergoing ICIs were collected from start to end of treatment (EoT). GM was profiled through Illumina, that is, 16S rRNA sequencing, and subsequently processed through a bioinformatics pipeline. The overall response rate to ICIs was 30.5%, with no association between patients clinical characteristics and response/survival outcomes. Regarding GM, responder patients showed a peculiar significant enrichment of *Lachnospira*, while non-responder ones showed higher presence of *Enterobacteriaceae* (at baseline and maintained till EoT). Recognizing patient-related factors that may influence response to ICIs is becoming critical to optimize the treatment pathway of heavily pretreated, young patients with a potentially long-life expectancy. These preliminary results indicate potential early GM signatures of ICIs response in lymphoma, which could pave the way for future research to improve patients prognosis with new adjuvant strategies.

KEYWORDS
adjuvant strategy, checkpoint inhibitors, gut microbiome, lymphoma, outcome

1 | INTRODUCTION

In the past decade, the host immune system has become a major focus of research because of its central role in the pathogenesis of cancer. Indeed, evasion of immune surveillance is one of the main mechanisms that cancer cells put in place for their survival and proliferation. In this setting, the use of immune checkpoint inhibitors (ICIs), particularly monoclonal antibodies (mAbs) directed against PD-1 (programmed cell death receptor-1, anti-PD1 mAbs), has shown good efficacy with a manageable safety profile for the

treatment of several B-cell malignancies, such as relapsed/refractory (r/r) classical Hodgkin lymphoma (cHL) and primary mediastinal B-cell lymphoma (PMBCL).[1–4] Although data show a significant anti-tumor efficacy with an overall response rate (ORR) ranging from 40% to 70% according to histology, more than half of these patients eventually progress or lose response, regardless of the underlying disease and the type of ICIs employed.[1–4]

Understanding the variability of response in patients with the same pathology and undergoing the same treatment is therefore a key point in hematological research with the aim of identifying strategies that can enhance the efficacy of ICIs and better predict patient outcomes. In this scenario, increasing attention is being paid to the gut microbiome (GM), the community of trillions of microorganisms, mainly bacteria but also eukaryotes, viruses and archaea, which inhabits the human gastrointestinal tract and profoundly influence human physiology.[5] In particular, since 2015, milestones have been reached on the role of GM in immunotherapy,[6,7] showing that the GM profile at diagnosis, as well as its temporal dynamics during anticancer treatments, could influence the response to therapies, modulating their efficacy and toxicity.[8–11] This influence is most likely due to the ability of GM to regulate immune responses through the production and/or activation of bacterial-derived molecules, the translocation of its members into the peripheral circulation, and the cross-reactivity with tumor antigens.[12] However, to our knowledge, most of the research in Hematology has focused on the impact of GM on the outcomes of cell-based therapies such as allogeneic hematopoietic stem cell transplantation (the risk and severity of graft-versus-host disease and overall survival [OS]),[13–15] and chimeric antigen T-cell therapy (the risk and severity of immune effector-cell associated toxicity and treatment response),[16,17] while data on the relationship between GM and ICIs response in lymphoma patients are still lacking.

Herein, we hypothesized that the GM configuration at baseline and its dynamics during treatment have an impact on the therapeutic response also in pretreated B-cell lymphoma patients scheduled for anti-PD1 mAbs. To test this assumption, we recruited adult patients with r/r cHL or PMBCL and profiled their GM before and during anti-PD1 therapy, until the end of treatment (EoT) or disease relapse or progression, whichever came first.

2 | MATERIALS AND METHODS

2.1 | Study design

A prospective, single-center, exploratory human GM study was conducted. Thirty patients (aged 18 years or older) with histologically confirmed r/r cHL or PMBCL who were candidates for single-agent anti-PD-1 therapy, namely pembrolizumab or nivolumab, were consecutively enrolled. Patients received nivolumab at a dose of 3 mg/kg or 240 mg every 2 weeks for up to 2 years or pembrolizumab at a fixed dose of 200 mg every 3 weeks for up to 2 years as per clinical practice, based on histology and previous lines of therapy.

Stool samples were collected at baseline, that is, 1 week before the first course of anti-PD1 treatment, and at each treatment cycle, till EoT or relapse or progression, whichever occurred first. Fecal samples were also collected in the event of gastrointestinal toxicity and/or immune-related adverse events (irAEs) grade ≥2 or any other non-hematological AEs grade 3 or higher. Hematological and non-hematological AEs were graded according to CTCAE v.4.0.

Disease assessments were performed using positron emission tomography and computed tomography scan at baseline and with subsequent timing as per clinical practice. Patients who discontinued treatment due to disease progression or grade 4 hematological toxicity and/or grade ≥3 non-hematologic toxicity were followed up for survival. Response was defined according to the 2014 Lugano classification.[18,19] ORR was defined as the sum of partial response (PR) and complete response (CR) rates at EoT, whereas best ORR was defined as the best response achieved at any timepoint after the initiation of ICIs. OS was calculated from the date of infusion until death from any cause or last available follow-up. Disease-free survival was estimated from the date of the first documented CR to the last follow-up or the date of disease recurrence or death as a result of lymphoma or acute toxicity of study treatment; progression-free survival (PFS) was defined as the time from infusion for all treated patients to the first observation of progressive disease or death from any cause.

The primary objective of the study was the longitudinal phylogenetic profiling of the GM of lymphoma patients treated with ICIs (before, during and at the EoT), while the secondary objectives were any associations between GM composition at baseline with response to ICIs and patient survival.

The study was approved by our institutional board (Ethical Committee AVEC of Bologna, approval id 015/2017/U/Tess/AOUBO). All participants gave written informed consent in accordance with the Declaration of Helsinki.

2.2 | 16S rRNA amplicon sequencing and data processing

Microbial DNA was extracted from fecal samples using the repeated bead-beating plus column method as previously described.[20] In brief, 250 mg of feces were resuspended in 1 mL of lysis buffer (500 mM NaCl, 50 mM Tris-HCl pH 8, 50 mM EDTA, 4% SDS [w/v]) with four 3-mm glass beads and 0.5 g of 0.1-mm zirconia beads, and mechanically homogenized thrice in a FastPrep instrument (MP Biomedicals) at 5 movements/s with a 1-min incubation period on ice every 5 min. Samples were then incubated at 95°C for 15 min and centrifuged to separate beads and stool particles. Ten molar ammonium acetate was added to the supernatants, and after 10-min incubation nucleic acids were precipitated by adding one volume of isopropanol. After a further centrifugation step, the pellets were washed with 70% ethanol and then resuspended in TE buffer (10 mM Tris-HCl, 1 mM EDTA pH 8). RNA and protein were removed by treatment with DNase-free RNase (10 mg/mL) at 37°C for 15 min and proteinase K

at 70°C for 10 min, respectively. DNA was then purified using the DNeasy Blood & Tissue Kit (QIAGEN).

For library preparation, the V3-V4 hypervariable regions of the 16S rRNA gene were amplified using primers 341F and 785R with Illumina overhang adapters according to the Illumina protocol "16S Metagenomic Sequencing Library Preparation" (Illumina). Amplicons were purified using a magnetic bead-based clean-up system (Agencourt AMPure XP; Beckman Coulter). The Nextera technology was then used for limited-cycle PCR to generate indexed libraries. The indexed amplicons were further purified and then pooled at equimolar concentration (4 nM). The pool was denatured with 0.2 N NaOH and diluted to 4.5 pM with a 20% PhiX control for paired-end sequencing (2 × 250 bp) on an Illumina MiSeq platform. Sequence reads were deposited in the National Center for Biotechnology Information Sequence Read Archive (NCBI SRA).

Raw amplicon sequences were analyzed using a bioinformatics pipeline combining PANDASeq and QIIME 2.[21,22] After length and quality filtering, reads were clustered into amplicon sequence variants (ASVs) using DADA2.[23] Chimeras were discarded during the process. The VSEARCH tool was used to assign taxonomy using the Greengenes database as a Reference [24]. Publicly available sequences from healthy subjects matched for GM-associated confounding factors (i.e., age, gender, and geography) were retrieved and used as controls. Sequences were obtained from: Schnorr and colleagues (deposited in the MG-RAST database: project ID mgp12183),[25] and Biagi and colleagues (MG-RAST database: project ID mgp17761).[26] All fecal samples were processed in the same laboratory, then subjected to the same wet and in silico analysis steps. The q2-diversity plugin was used to perform alpha and beta diversity assessments. The Shannon diversity index, an alpha diversity metric, was used to assess intra-sample richness and evenness of microbial taxa. principal coordinates analysis (PCoA) graphs were then constructed utilizing Bray–Curtis and weighted and unweighted UniFrac distances to assess the (dis)similarities between samples, representing beta diversity.

The PICRUSt 2.0 (v2.5.0) prediction tool was used to profile the baseline gut microbiota pathway composition of the patients.[27] The ASVs and the BIOM table with ASV abundance across the samples were used as input. The predicted MetaCyc pathway abundances were then normalized to relative abundances. To obtain the corresponding names and descriptions, we searched the pathway IDs in the MetaCyc database.

2.3 | Statistical analysis

As no preliminary data on the same matter of the present project were available in literature, no formal sample size estimation was made. On the basis of the case histories of the hospital involved in the project and taking into account an enrollment period of 12 months, we foreseen to enroll 30 patients. Patients' demographics and characteristics were summarized by descriptive statistics.

Comparisons between groups were performed using contingency table analysis with chi-squared or Fisher's exact test for categorical variables, as appropriate, whereas continuous data were analyzed using Student's *t* test, after checking for normal distribution (based on the Shapiro–Wilk statistic), or otherwise the Wilcoxon rank-sum test. Statistical analyses for clinical data were performed using Stata 17 (StataCorp LP).

For GM data, all statistical analyses were performed using R software (https://www.R-project.org/). The Wilcoxon test was used to assess differences in GM composition (i.e., relative taxon abundance) and alpha diversity between study groups. The ggplot2 and ggsignif packages were used to generate boxplots. PCoA plots were constructed using the vegan package for multidimensional scaling, and pairwise Adonis was used to test for data separation using a permutation test with pseudo-*F* ratio.[28] The point-biserial correlation test was used to evaluate associations between therapeutic response and relative taxon abundances. In case of significant association, Spearman's correlation test was then used to evaluate the associations between relative taxon abundances and nutritional values. Heatmaps where plotted using taxa or pathway relative abundances and the variables were hierarchical clustered and sorted according to their Euclidean distances.

A $p \leq 0.05$ was considered statistically significant.

3 | RESULTS

3.1 | Clinical outcomes and safety

Thirty patients were consecutively enrolled, 20 of whom were evaluable for study objectives, while 10 were excluded from the analysis mainly due to withdrawal of consent, lack of stool sample at baseline, and rapid disease progression resulting in treatment modification. Of the 20 evaluable patients, 5 were affected by PMBCL while 15 had cHL. Fourteen patients were female and 6 were male. The median age at enrollment was 28.5 years (18.3–71.4). Eleven patients (55%) had stage III/IV, according to Ann Arbor classification, with 45% of patients presenting with extra-nodal disease involvement. The median number of lines of therapy failed before ICIs was 3 (2–8), with 15 patients (75%) being refractory to the first line of treatment and all except one being refractory to the last line of treatment before ICIs. Regarding previous therapies, patients were treated in a homogeneous manner in accordance with the therapeutic indications for each disease. The median time from last therapy to the first infusion of ICIs was 46 days (8–179) with a statistically significant difference between patients with cHL (46 days) and PMBCL (66 days) ($p < 0.05$) (Table S1).

For 8 patients (all with cHL), the scheduled therapy was nivolumab, while 12 patients (7 with cHL and all PMBCL patients) received pembrolizumab. The median number of drug cycles was 14 (1–39), specifically, 16 cycles (6–39) for nivolumab and 9 for pembrolizumab (1–35). There was a significant difference between

patients with cHL and those with PMBCL, as the latter had a median of 4 cycles of therapy before interruption ($p < 0.05$) (Table S1). All patients discontinued treatment early, the main causes being disease progression (11 patients) and achievement of complete remission (4 patients), subsequently consolidated with a stem cell transplantation.

At first restaging, after 4 cycles of treatment, 5 (20.5%) patients were in CR (3 with cHL and 2 with PMBCL), 6 (30%) were in PR (all with cHL), while 6 had a disease progression (4 with cHL and 2 with PMBCL). During the course of therapy, 2 patients in PR converted their response to CR, while the remaining 4 patients in PR progressed. At final evaluation, 30% of patients were in CR (4 with cHL and 2 with PMBCL) and 1 was in PR (converted from stable disease) achieving an ORR of 30.5%. The best ORR was 60%, with 6 patients (30%) in CR and 6 (30%) in PR, as the best response (Table S2).

In terms of safety, 26 non-hematological treatment-related AEs occurred, predominantly grade 1–2. Seven irAEs were recorded, mainly grade 1–2 thyroiditis. Three patients developed 6 hematological AEs, with grade 1–2 anemia and thrombocytopenia being the most frequent.

Regarding concomitant medications, patients did not undergo antibiotic therapy right neither before nor during ICIs treatment.

With a median follow-up of 28.9 months, the median PFS and OS for the entire population were 11 and 41.3 months, respectively. Based on histology, median PFS was 11.1 months for cHL patients and 23.5 months for PMBCL patients, while median OS was 41.5 months and not reached, respectively. No associations were found between patients' baseline clinical characteristics and outcomes (best response, final response and OS).

3.2 | GM dysbiosis of B-cell lymphoma patients before ICIs treatment compared to healthy subjects

The baseline GM structure of evaluable patients was compared with that of healthy age/gender-matched Italian subjects as controls (Table S3). Alpha diversity, as assessed by the Shannon index, was lower in patients than in controls ($p = 0.02$; Wilcoxon test) (Figure 1A). As for beta diversity, PCoA based on Bray–Curtis distances, showed significant segregation between the two study groups ($p = 0.0001$; adonis) (Figure 1B). The two groups also differed in the relative abundance of many taxa, even at the phylum level. Specifically, the phylum Actinobacteria was overrepresented in patients ($p = 0.01$; Wilcoxon test), whereas Verrucomicrobia and Tenericutes were overrepresented in controls ($p \leq 0.04$) (Figure 1C). At the family level (Figure 1D), patients were discriminated by a higher relative abundance of *Streptococcaceae*, *Coriobacteriaceae*, and *Erysipelotrichaceae*, while lower of *Bifidobacteriaceae*, *Rikenellaceae*, *Porphyromonadaceae*, *Verrucomicrobiaceae*, *Ruminococcaceae*, and *Lachnospiraceae* ($p \leq 0.02$). Furthermore, the family *Bacteroidaceae* tended to be underrepresented in patients ($p = 0.06$). At the genus level (Figure 1E and Figure S1), the patient group showed a reduced

relative abundance of *Bifidobacterium*, *Parabacteroides*, *Odoribacter*, *Akkermansia*, *Clostridium*, *Anaerostipes*, *Coprococcus*, *Lachnobacterium*, *Dehalobacterium*, *Blautia*, *Dorea*, *Lachnospira*, *Roseburia*, *Faecalibacterium*, *Anaerotruncus*, *Ruminococcus*, *Bilophila*, and *Sutterella*, while a higher relative abundance of *Streptococcus* ($p \leq 0.04$). In addition, patients tended to be depleted in *Bacteroides*, *Butyricimonas* and *Coprobacillus*, while enriched in *Collinsella* ($p \leq 0.07$).

The diminished microbial diversity observed in patients, marked by the depletion of health-associated commensal taxa and the proliferation of potentially pathogenic bacteria—recognized as dysbiosis—can be attributed to a multifaceted interplay of factors. These factors encompass prior treatments, antibiotic exposure, alterations in lifestyle, and the intrinsic nature of the disease itself. Collectively, these observations suggest that the GM of our patients exhibited disruption compared to that of healthy controls, a perturbation evident even before the initiation of ICIs treatment.

3.3 | Potential GM signatures predictive of ICIs treatment outcomes

Patients were stratified into responders, that is, those who achieved CR or PR, and non-responders, that is, those who maintained a stable disease or progressed, based on the final assessment, and their baseline and EoT GM structures were compared. No significant differences in term of alpha and beta diversity were found between the two groups both at baseline and EoT (Figures 2A,B and 3A,B), while from a taxonomic point of view (Figures 2C–E and 3C–E) several distinctive features emerged. In particular, prior to starting treatment with ICIs, responder patients were distinguished by a higher relative abundance of *Lachnospiraceae* and *Lachnospira* ($p \leq 0.04$), and showed a trend toward increased proportions of *Peptostreptococcaceae* and *Prevotellaceae*, along with the genus *Prevotella* ($p \leq 0.06$). The baseline relative abundance of *Lachnospiraceae* and *Lachnospira* correlated positively with the ORR (rpb = 0.59 and 0.62, $p = 0.03$ and 0.02, respectively) (Figure 2F). On the other hand, non-responder patients showed a higher relative abundance of Proteobacteria and *Enterobacteriaceae* ($p \leq 0.04$), and a trend toward a higher representation of *Lactobacillaceae*, especially *Lactobacillus* ($p = 0.07$). To evaluate the potential confounding effects of sex, age and disease on the predictive GM signature, we evaluated beta diversity and the genus-level relative abundances among these groups at baseline. Results are presented in Figures S2-S4.

At EoT (Figure 3A–E), the previously identified potential GM signatures of response were largely maintained, namely the overrepresentation of *Lachnospiraceae* in responders, and the overrepresentation of Proteobacteria, *Enterobacteriaceae* and *Lactobacillus* in non-responders ($p \leq 0.095$). Furthermore, responder subjects showed higher proportions of Firmicutes ($p = 0.03$) and a trend toward an increase in *Ruminococcus* ($p = 0.085$). The relative abundance of *Lachnospiraceae* and *Ruminococcus* at EoT correlated positively with ORR (rpb = 0.73, $p = 0.03$) (Figure 3F).
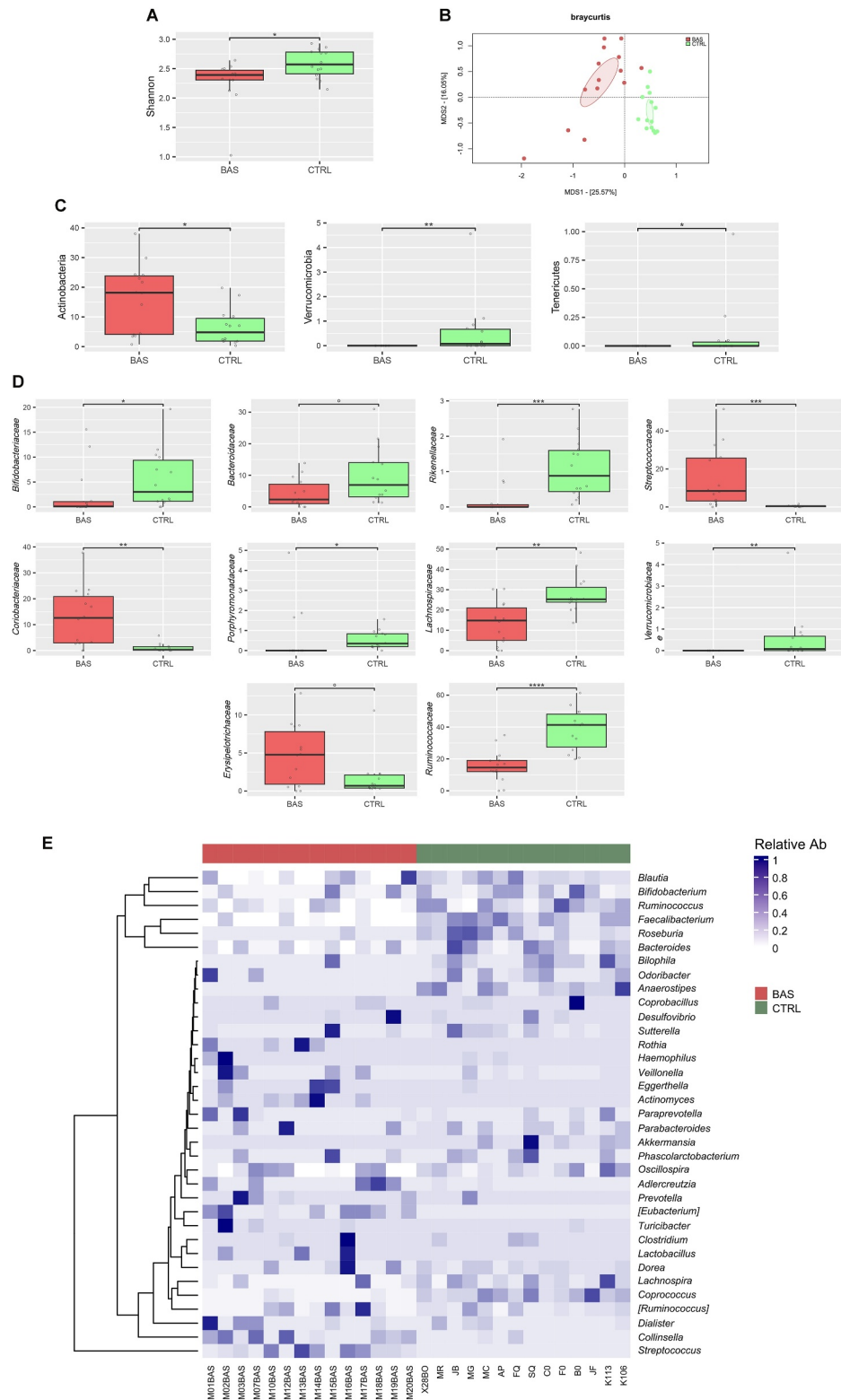
FIGURE 1 Legend on next page.

3.4 | Predicting functional microbiome pathways potentially involved in patients ICIs outcome

From the PICRUSt2-predicted MetaCyc pathways of patient's GM at baseline, we evaluated the relative abundance of these pathways in relation to the patient's therapy outcomes to identify potential predictive functional signatures. Differences in pathways abundances between responders (R) and non-responders (NR) were determined using the Wilcoxon test. We found that certain pathways were significantly increased in the R group ($p \leq 0.036$). These include D-

galacturonate degradation (GALACTUROCAT-PWY), glycogen degradation I (GLYCOCAT-PWY), superpathway of L-serine and glycine biosynthesis I (SER-GLYSYN-PWY), biotin biosynthesis II (PWY-5005). These pathways are associated with enhanced metabolic and biosynthetic capabilities, potentially supporting the energy demands and biosynthesis of essential compounds required for an effective immune response and modulation. Conversely, the GM of NR was characterized by a predominance of fermentative metabolism pathways, such as the superpathway of hexitol degradation (bacteria) (HEXITOLDEGSUPER-PWY), hexitol fermentation to lactate, formate, ethanol, and acetate (P461-PWY), and the superpathway of glycolysis and Entner-Doudoroff (GLYCOLYSIS-E-D) ($p \leq 0.036$). These pathways indicate a metabolic shift toward fermentation, which may lead to the production of metabolites that can create a more inflammatory or less immune-supportive environment. All significant associations ($p \leq 0.05$) are reported in Figure 4, providing a comprehensive view of how these microbial pathways might influence patient responses to ICIs.

4 | DISCUSSION

In our exploratory study, we longitudinally profiled the GM of adult patients with r/r cHL or PMBCL undergoing anti-PD-1 therapy (nivolumab or pembrolizumab) in an attempt to identify potential predictive GM signatures of ICIs response. Although the enrolled patients were heavily pretreated (median number of previous lines, 3) and had advanced disease, refractory to the last line prior to ICIs, response rates and survival were comparable to those reported in the literature. In particular, the best response in cHL patients was 67% with a median PFS of 11.1 months, similar to the results of the Keynote-087 and Checkmate-205 studies.[1,2] Regarding patients with PMBCL, 40% achieved a response with a median PFS of almost 2 years, a result significantly different from the median PFS of 4.3 months reported in the Keynote-170 study.[3] However, this finding may be influenced by the small sample size of our study.

Considering that cancer patients' GM, including those with B-cell non-Hodgkin's lymphomas, is altered both at the time of diagnosis,[29–31] underscoring a close correlation between disease onset and loss of GM diversity, and following previous treatment,[13–17] we first compared the baseline GM profiles of patients with those of healthy subjects matched for microbiota-associated confounding factors (i.e., age, gender, and geography),[32] indicating that, also in our cohort of r/r B-cell lymphoma patients, the GM prior to the initiation of ICIs treatment is dysbiotic. In particular, it showed predictably low diversity and an unbalanced composition, with enrichment in potential pathobionts, for example, *Streptococcus* and *Collinsella* and depletion of typical health-associated taxa, including *Bifidobacterium* and members of the *Lachnospiraceae* and *Ruminococcaceae* families (e.g., *Coprococcus, Lachnobacterium, Blautia, Dorea, Lachnospira, Roseburia, Faecalibacterium,* and *Ruminococcus*).[33–37] As widely discussed in the literature, the latter are known to produce short-chain fatty acids (SCFAs), end-products of fiber fermentation, which are key players in promoting metabolic and immunological homeostasis.[38]

Notably, a baseline dysbiotic signatures were less pronounced in those patients in our cohort who subsequently responded to therapy. In particular, we found potential GM signatures, characterizing both baseline and EoT samples, able to segregate responder patients from non-responder ones. Specifically, prior to ICIs treatment, responder subjects showed an overrepresentation of *Lachnospiraceae* and *Prevotellaceae* (and the respective genera *Lachnospira* and *Prevotella*), and an underrepresentation of Proteobacteria (especially *Enterobacteriaceae*) and *Lactobacillus* compared to non-responders. Most of these taxa continued to discriminate between responder and non-responder patients at EoT. Supporting the potential role of these microorganisms in influencing ICIs efficacy, the relative abundance of *Lachnospiraceae* and *Lachnospira* at baseline was positively correlated with ORR, as was the relative abundance of *Lachnospiraceae* and *Ruminococcus* at EoT. As we already know, *Lachnospiraceae* and *Ruminococcus* are capable of producing SCFAs, mainly butyrate, which can enhance the antitumoral activity of the immune system by modulating the function of several immune cells such as macrophages, dendritic cells, anti-inflammatory T-regulatory cells, pro-inflammatory T helper cells and plasma cells.[39,40]

Regarding the other discriminating taxa, the response-associated depletion of *Enterobacteriaceae* was expected, as their enrichment has already been correlated with unfavorable outcomes in naïve diffuse large B-cell lymphomas.[31] In contrast, the potential role we found of *Prevotella* and *Lactobacillus* as a favorable and unfavorable prognostic factor, respectively, partially contradicts the available literature,

FIGURE 1 Gut microbiota dysbiosis of B-cell lymphoma patients before ICI treatment compared to healthy subjects. (A) Boxplots showing the distribution of alpha diversity, estimated according to the Shannon index, in the gut microbiota of B-cell lymphoma patients before ICI treatment (BAS) versus healthy age/gender-matched Italian subjects (CTRL). A significant decrease in alpha diversity is observed in the patient group ($p = 0.02$; Wilcoxon test). (B) Principal coordinates analysis based on Bray–Curtis distances between study groups. Ellipses include 95% confidence area based on the standard error of the weighted average of sample coordinates. The analysis reveals significant segregation between the microbiota of patients and healthy subjects ($p = 0.0001$; adonis), indicating distinct microbial community structures. Boxplots showing the relative abundance distribution of (C) phyla and (D) families differentially represented between patients and healthy subjects. °$p \leq 0.1$; *$p \leq 0.05$; **$p \leq 0.01$; **$p \leq 0.001$; ****$p \leq 0.0001$; Wilcoxon test. (E) Heatmap showing relative abundance differences, scaled by row, of the more abundant and prevalent GM genera (relative abundance $\geq 0.1\%$ in at least 1/8 of the studied population) between R and NR patients at baseline. Only pathways showing significant differences ($p \leq 0.05$; Wilcoxon test) between groups are plotted. Pathways are hierarchical clustered and sorted according to their Euclidean distances. GM, gut microbiome; ICI, immune checkpoint inhibitor; NR, non-responder; R, responder.
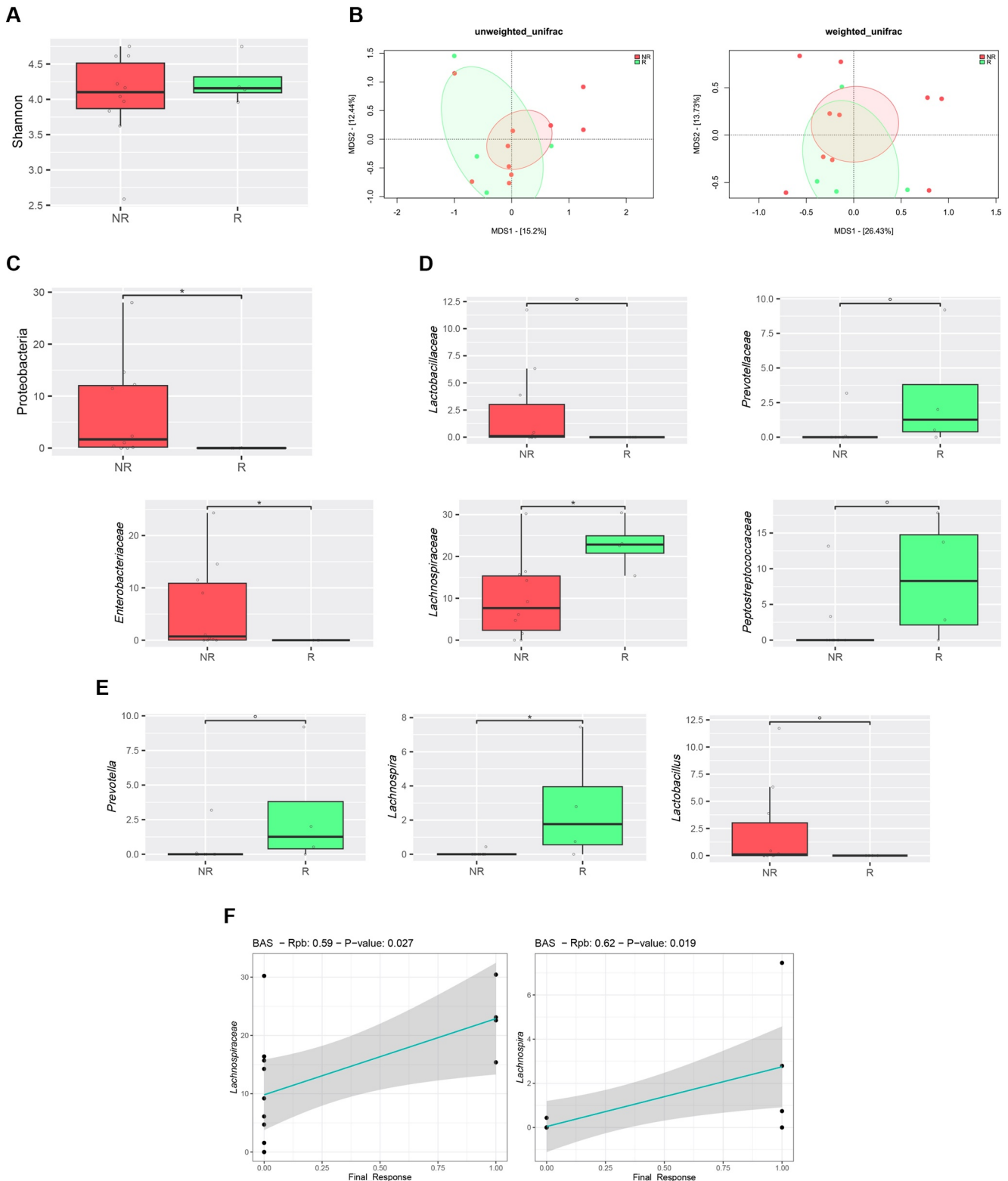
FIGURE 2 Potential gut microbiota signatures of response to ICIs in B-cell lymphoma patients at baseline. (A) Boxplots showing the distribution of alpha diversity, estimated according to the Shannon index, in the baseline gut microbiota profile of B-cell lymphoma patients stratified by response (R, responders vs. NR, non-responders). The analysis reveals no significant differences in alpha diversity between R and NR ($p = 0.73$; Wilcoxon test). (B) PCoA based on unweighted and weighted UniFrac distances between study groups. The PCoA shows no significant segregation between R and NR ($p > 0.05$; adonis). Ellipses include the 95% confidence area based on the standard error of the weighted average of sample coordinates, indicating overlapping microbial community structures between the two groups. Boxplots showing the relative abundance distribution of (C) phyla, (D) families, and (E) genera differentially represented between groups. °$p \leq 0.1$, *$p \leq 0.05$; Wilcoxon test. (F) Scatterplots showing the point-biserial correlation (rpb) between relative taxon abundances and ORR. Only significant correlations ($p \leq 0.05$) with absolute rpb ≥ 0.3 are shown, identifying taxa that are strongly associated with treatment response. ICIs, immune checkpoint inhibitors; ORR, overall response rate; PCoA, principal coordinates analysis.
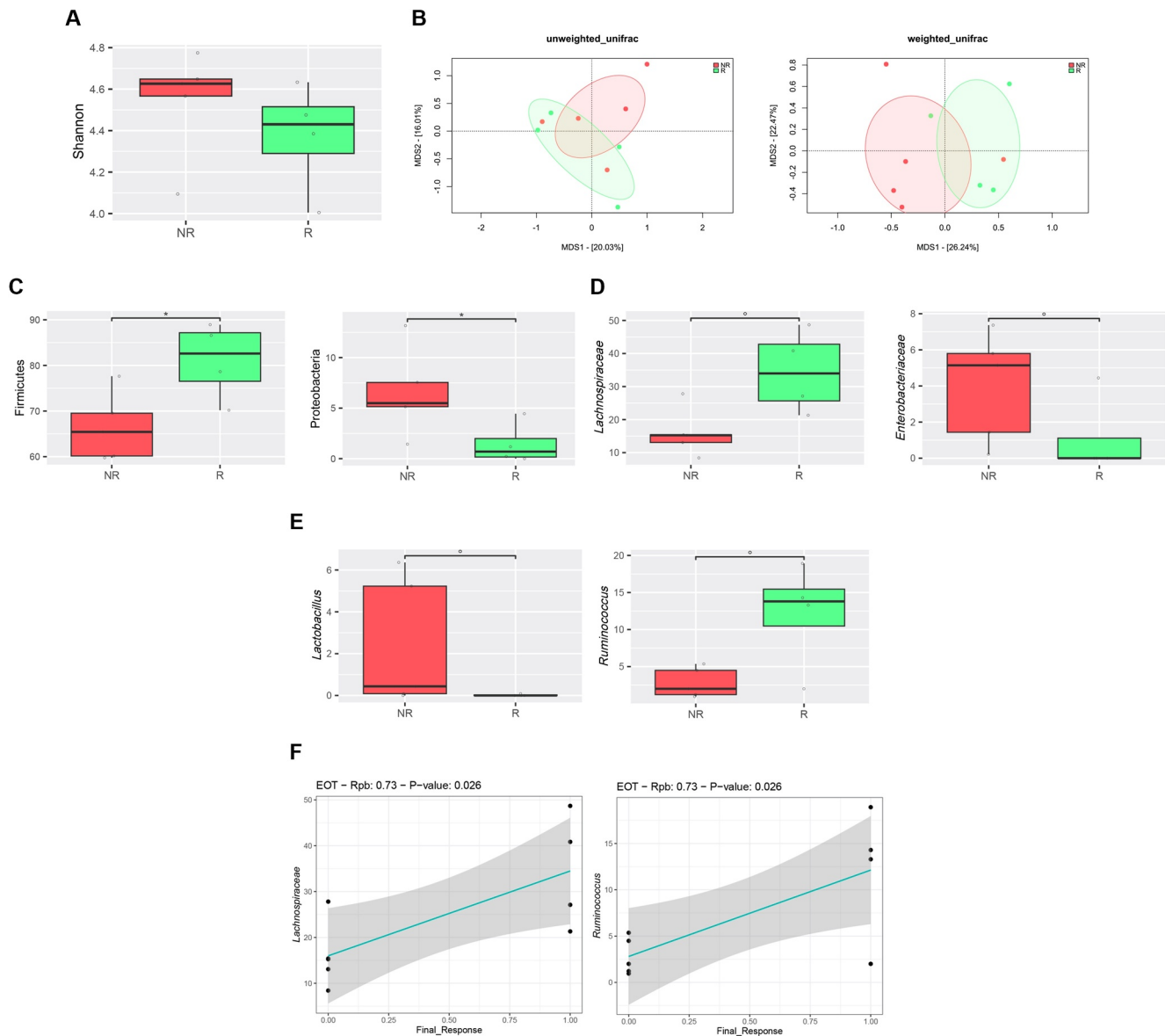
FIGURE 3 Differences in the gut microbiota profile of B-cell lymphoma patients at the end of ICI treatment according to response. (A) Boxplots showing the distribution of alpha diversity, estimated according to the Shannon index, in the gut microbiota of B-cell lymphoma patients stratified by response (R, responders vs. NR, non-responders) at the end of ICI treatment. The analysis reveals no significant differences between R and NR ($p = 0.29$; Wilcoxon test). (B) PCoA based on unweighted and weighted UniFrac distances between study groups. The PCoA shows no significant segregation between R and NR ($p \geq 0.05$; adonis). Ellipses include 95% confidence area based on the standard error of the weighted average of sample coordinates, indicating that the microbial community structures are similar between the two groups. Boxplots showing the relative abundance distribution of (C) phyla, (D) families, and (E) genera differentially represented between groups, suggesting changes in the gut microbiota composition and potential microbial markers of response. °$p \leq 0.1$, *$p \leq 0.05$; Wilcoxon test. (F) Scatterplots showing the point-biserial correlation (rpb) between relative taxon abundances and ORR. Only significant ($p \leq 0.05$) correlations with absolute rpb ≥ 0.3 are shown, identifying taxa that are strongly associated with treatment response. ICI, immune checkpoint inhibitor; ORR, overall response rate; PCoA, principal coordinates analysis.

which generally reports the former as associated with cancer progression, and the latter as a probiotic taxon.[41,42] However, it should be noted that *Lactobacillus* has recently been identified among genera that were overrepresented in B-cell lymphoma patients with high disease burden or chemotherapy-related side effects,[43] suggesting a potential species- and context-dependent role. It is important to note that while *p* values did not reach conventional levels of statistical

significance, they are still meaningful to report statistical tendencies or trends when discussing microbiome data.[44,45] In our study, this observation suggests a potential trend toward depletion, which warrants further investigation or consideration in the context of broader research findings.

We investigated potential confounding effects of age, sex and disease type on the GM signatures predictive of ICIs therapy
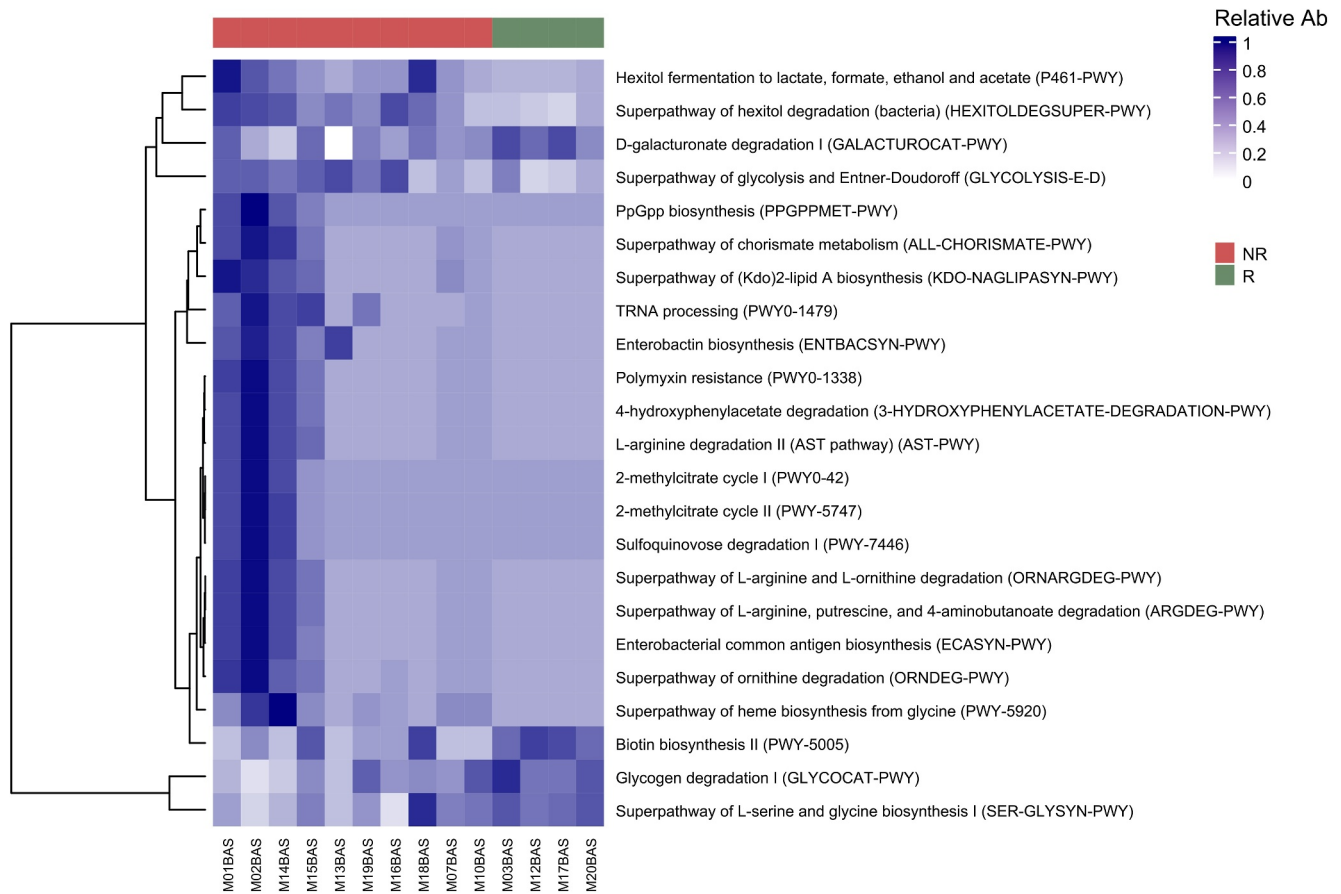
FIGURE 4 Predicted gut microbiota pathway relative abundance differences at baseline according to overall response rate. Heatmap showing relative abundance differences, scaled by row, in the gut microbiome PICRUSt2-predicted MetaCyc pathway between responder (R) and non-responder (NR) patients at the baseline. Only pathways with significant differences ($p \leq 0.05$; Wilcoxon test) between groups are plotted, suggesting potential biomarkers for predicting response to ICIs treatment in B-cell lymphoma patients. Pathways are hierarchical clustered and sorted according to their Euclidean distances. ICIs, immune checkpoint inhibitors; NR, non-responder; R, responder.

outcomes in B-cell lymphoma patients. Our analyses revealed age as a potential confounding factor, notably affecting the relative abundance of the *Lachnospira* genus, which showed an age-related increase in older subjects at baseline, particularly prevalent among responders (Figure S2). Sex did not significantly influence GM signatures, while differences in GM composition between different lymphoma types (i.e., PMBCL and cHL) did not align with ICIs therapy outcome signatures. These findings underscore the importance of considering age-related GM changes when interpreting microbial predictors of ICIs treatment response, suggesting avenues for future research to refine predictive models.

To deeply understand the impact of the microbiota on patient prognosis, we predicted the functional potential of the patient's microbiome using the PICRUSt2 package based on 16S rRNA sequencing data. This prediction provides a more comprehensive overview of the possible involvement of gut microbiota in anti-PD1 therapy. The network of microbial pathways present in a patient's microbiota could support a healthy and balanced gut environment, thereby enhancing the efficacy of ICIs such as anti-PD1 mAbs by promoting better immune cell function and response. Enhanced pathways in the R group, such as D-galacturonate degradation and

glycogen degradation I, suggest an increased availability of energy sources. These pathways support the production of SCFAs, which are known for their anti-inflammatory properties, ability to modulate the immune system, and role in strengthening the gut barrier.[37,46] SCFAs like butyrate are critical for maintaining gout homeostasis and supporting the differentiation of regulatory T cells, which can enhance the immune response against tumors. The superpathway of L-serine and glycine biosynthesis I and biotin biosynthesis II are also significantly increased in the R group. L-serine and glycine are amino acids essential for nucleotide synthesis and other metabolic processes vital for rapidly proliferating cells, including immune cells.[47,48] Biotin, a B-vitamin, is crucial for various carboxylation reactions, which play a role in gluconeogenesis, fatty acid synthesis, and amino acid catabolism. Enhanced biotin biosynthesis may thus support the metabolic demands of activated immune cells during ICIs therapy.

Conversely, the predominance of fermentative metabolism pathways in NRs, such as hexitol fermentation and glycolysis, may lead to the production of metabolites that can adversely affect the gut environment and immune response. Ethanol, produced from hexitol fermentation, can increase oxidative stress and disrupt the gut barrier, potentially leading to a pro-inflammatory state detrimental to

effective immune responses. Formate, another bacterial fermentation product, can contribute to metabolic acidosis and inhibit cellular respiration, further compromising immune cell function.[49]

Our results suggest that GM functional profiling could be crucial to better elucidate the role of the GM in patients' responses to ICIs therapy and the molecular mechanism involved. Understanding these associations can inform the development of microbiome-based interventions to improve therapeutic outcomes.

Nevertheless, our study is not without limitations. First of all, the small size of the patient cohort, that constrained the robustness of the statistical evaluations. Additionally, the comparison of baseline GM between patients and controls may have been influenced by potential biases introduced by prior lines of lymphoma treatment and previous antibiotic exposure. In fact, patients did not undergo antibiotics right before or during therapy eliminating them from the list of potential confounding factors, but we did not have information about antibiotics in previous medical history of both patients and controls. Importantly, recognizing and addressing the potential confounding effects of previous treatments on baseline GM comparisons will be crucial for a more nuanced understanding of the study results. Finally, longitudinal sampling was not consistent across patients, preventing a robust high-resolution assessment of GM trajectories in responder versus non-responder patients, including in relation to AEs. To date, we conceived the study with fixed timepoints to ensure the consistency of longitudinal sampling, also for AE. Unfortunately, since these were fragile patients, the established timepoints were not always respected. In addition, due to the outpatient setting it was often impossible collect fecal samples contextually to an AE. These limitations underscore the need for caution in interpreting the findings and emphasize the importance of larger, more diverse samples to increase the study's statistical power and generalizability.

Despite the constrained size of our patient cohort, our study represents a pioneering effort to unravel GM signatures in patients with r/r cHL and PMBCL before initiating ICI treatment. In particular, we identified potential early prognostic GM biomarkers and in terms of a correlation between them and patient outcomes during anti-PD1 mAb therapy. These preliminary results open promising avenues for future research in this direction with the aim of optimizing response to ICIs in heavily pretreated patients affected by r/r cHL and PMBCL. The study was conceived as pivotal as there were no data exploring connections between GM, lymphomas and ICIs treatment. Our early results have to be considered as a start of point for further and more robust research. Moving forward, leveraging shotgun metagenomic sequencing will be crucial to uncover species-level variations and functional signatures within the GM of patients in response to ICIs treatments. By integrating species-level and functional analyses, future studies can more precisely delineate microbial signatures associated with therapy outcomes, thereby advancing our understanding and potentially enhancing clinical strategies in B-cell lymphoma treatment. This, in turn, will set the stage for a more tailored and personalized approach to treatment strategies in this challenging patient population. The prospects offered by understanding and manipulating the interplay between GM and immunotherapy outcomes underscore the evolving landscape of precision medicine in lymphoma treatment.

AUTHOR CONTRIBUTIONS

ACKNOWLEDGMENTS

CONFLICT OF INTEREST STATEMENT

The authors declare that they have no conflict of interest.

DATA AVAILABILITY STATEMENT

The data underlying this article are available from the corresponding author upon reasonable request.

ETHICS STATEMENT

The study was approved by the Ethics Committee AVEC of Bologna (approval id 015/2017/U/Tess/AOUBO) and was conducted in accordance with the Declaration of Helsinki.

ORCID

Lisa Argnani 🔟 https://orcid.org/0000-0003-4225-4626
Pier Luigi Zinzani 🔟 https://orcid.org/0000-0002-2112-2651

PEER REVIEW

The peer review history for this article is available at https://www.webofscience.com/api/gateway/wos/peer-review/10.1002/hon.3301.

REFERENCES

1. Ansell SM, Bröckelmann PJ, von Keudell G, et al. Nivolumab for relapsed/refractory classical Hodgkin lymphoma: 5-year survival from the pivotal phase 2 CheckMate 205 study. *Blood Adv*. 2023;7(20):6266-6274. https://doi.org/10.1182/bloodadvances.2023010334

2. Armand P, Zinzani PL, Lee HJ, et al. Five-year follow-up of KEYNOTE-087: pembrolizumab monotherapy for relapsed/refractory classical Hodgkin lymphoma. *Blood*. 2023;142(10):878-886. https://doi.org/10.1182/blood.2022019386

3. Zinzani PL, Thieblemont C, Melnichenko V, et al. Pembrolizumab in relapsed or refractory primary mediastinal large B-cell lymphoma:

final analysis of KEYNOTE-170. *Blood.* 2023;142:141-145. https://doi.org/10.1182/blood.2022019340

4. Zinzani PL, Santoro A, Gritti G, et al. Nivolumab combined with brentuximab vedotin for R/R primary mediastinal large B-cell lymphoma: a 3-year follow-up. *Blood Adv.* 2023;7(18):5272-5280. https://doi.org/10.1182/bloodadvances.2023010254

5. Turroni S, Brigidi P, Cavalli A, Candela M. Microbiota-host transgenomic metabolism, bioactive molecules from the inside. *J Med Chem.* 2018;61(1):47-61. https://doi.org/10.1021/acs.jmedchem.7b00244

6. Sivan A, Corrales L, Hubert N, et al. Commensal *Bifidobacterium* promotes antitumor immunity and facilitates anti-PD-L1 efficacy. *Science.* 2015;350(6264):1084-1089. https://doi.org/10.1126/science.aac4255

7. Vétizou M, Pitt JM, Daillère R, et al. Anticancer immunotherapy by CTLA-4 blockade relies on the gut microbiota. *Science.* 2015;350(6264):1079-1084. https://doi.org/10.1126/science.aad1329

8. Gopalakrishnan V, Helmink BA, Spencer CN, Reuben A, Wargo JA. The influence of the gut microbiome on cancer, immunity, and cancer immunotherapy. *Cancer Cell.* 2018;33(4):570-580. https://doi.org/10.1016/j.ccell.2018.03.015

9. Routy B, Le Chatelier E, Derosa L, et al. Gut microbiome influences efficacy of PD-1-based immunotherapy against epithelial tumors. *Science.* 2018;359(6371):91-97. https://doi.org/10.1126/science.aan3706

10. Matson V, Fessler J, Bao R, et al. The commensal microbiome is associated with anti-PD-1 efficacy in metastatic melanoma patients. *Science.* 2018;359(6371):104-108. https://doi.org/10.1126/science.aao3290

11. Wang Y, Jenq RR, Wargo JA, Watowich SS. Microbiome influencers of checkpoint blockade-associated toxicity. *J Exp Med.* 2023;220(3):e20220948. https://doi.org/10.1084/jem.20220948

12. Chamoto K, Yaguchi T, Tajima M, Honjo T. Insights from a 30-year journey: function, regulation and therapeutic modulation of PD1. *Nat Rev Immunol.* 2023;23(10):682-695. https://doi.org/10.1038/s41577-023-00867-9

13. Peled JU, Gomes ALC, Devlin SM, et al. Microbiota as predictor of mortality in allogeneic hematopoietic-cell transplantation. *N Engl J Med.* 2020;382(9):822-834. https://doi.org/10.1056/nejmoa1900623

14. Khuat LT, Dave M, Murphy WJ. The emerging roles of the gut microbiome in allogeneic hematopoietic stem cell transplantation. *Gut Microb.* 2021;13(1):1966262. https://doi.org/10.1080/19490976.2021.1966262

15. Masetti R, Leardini D, Muratore E, et al. Gut microbiota diversity before allogeneic hematopoietic stem cell transplantation as a predictor of mortality in children. *Blood.* 2023;142(16):1387-1398. https://doi.org/10.1182/blood.2023020026

16. Stein-Thoeringer CK, Saini NY, Zamir E, et al. A non-antibiotic-disrupted gut microbiome is associated with clinical responses to CD19-CAR-T cell cancer immunotherapy. *Nat Med.* 2023;29(4):906-916. https://doi.org/10.1038/s41591-023-02234-6

17. Smith M, Dai A, Ghilardi G, et al. Gut microbiome correlates of response and toxicity following anti-CD19 CAR T cell therapy. *Nat Med.* 2022;28(4):713-723. https://doi.org/10.1038/s41591-022-01702-9

18. Cheson BD, Fisher RI, Barrington SF, et al. Recommendations for initial evaluation, staging, and response assessment of Hodgkin and non-Hodgkin lymphoma: the Lugano classification. *J Clin Oncol.* 2014;32(27):3059-3068. https://doi.org/10.1200/jco.2013.54.8800

19. Cheson BD, Ansell S, Schwartz L, et al. Refinement of the Lugano Classification lymphoma response criteria in the era of immunomodulatory therapy. *Blood.* 2016;128(21):2489-2496. https://doi.org/10.1182/blood-2016-05-718528

20. Barone M, Garelli S, Rampelli S, et al. Multi-omics gut microbiome signatures in obese women: role of diet and uncontrolled eating behavior. *BMC Med.* 2022;20(1):500. https://doi.org/10.1186/s12916-022-02689-3

21. Masella AP, Bartram AK, Truszkowski JM, Brown DG, Neufeld JD. PANDAseq: paired-end assembler for illumina sequences. *BMC Bioinf.* 2012;13(1):31. https://doi.org/10.1186/1471-2105-13-31

22. Bolyen E, Rideout JR, Dillon MR, et al. Reproducible, interactive, scalable and extensible microbiome data science using QIIME 2. *Nat Biotechnol.* 2019;37(8):852-857. https://doi.org/10.1038/s41587-019-0209-9

23. Callahan BJ, McMurdie PJ, Rosen MJ, Han AW, Johnson AJ, Holmes SP. DADA2: high-resolution sample inference from Illumina amplicon data. *Nat Methods.* 2016;13(7):581-583. https://doi.org/10.1038/nmeth.3869

24. McDonald D, Price MN, Goodrich J, et al. An improved Greengenes taxonomy with explicit ranks for ecological and evolutionary analyses of bacteria and archaea. *ISME J.* 2012;6(3):610-618. https://doi.org/10.1038/ismej.2011.139

25. Schnorr SL, Candela M, Rampelli S, et al. Gut microbiome of the Hadza hunter-gatherers. *Nat Commun.* 2014;5(1):3654. https://doi.org/10.1038/ncomms4654

26. Biagi E, Franceschi C, Rampelli S, et al. Gut microbiota and extreme longevity. *Curr Biol.* 2016;26(11):1480-1485. https://doi.org/10.1016/j.cub.2016.04.016

27. Douglas GM, Maffei VJ, Zaneveld JR, et al. PICRUSt2 for prediction of metagenome functions. *Nat Biotechnol.* 2020;38(6):685-688. https://doi.org/10.1038/s41587-020-0548-6

28. Martinez Arbizu P. pairwiseAdonis: pairwise multilevel comparison using adonis. R package version 0.4. 2020.

29. Diefenbach CS, Peters BA, Li H, et al. Microbial dysbiosis is associated with aggressive histology and adverse clinical outcome in B-cell non-Hodgkin lymphoma. *Blood Adv.* 2021;5:1194-1198. https://doi.org/10.1182/bloodadvances.2020003129

30. D'Amico F, Decembrino N, Muratore E, et al. Oral lactoferrin supplementation during induction chemotherapy promotes gut microbiome eubiosis in pediatric patients with hematologic malignancies. *Pharmaceutics.* 2022;14(8):1705. https://doi.org/10.3390/pharmaceutics14081705

31. Yoon SE, Kang W, Choi S, et al. The influence of microbial dysbiosis on immunochemotherapy-related efficacy and safety in diffuse large B-cell lymphoma. *Blood.* 2023;141:2224-2238. https://doi.org/10.1182/blood.2022018831

32. Vujkovic-Cvijin I, Sklar J, Jiang L, Natarajan L, Knight R, Belkaid Y. Host variables confound gut microbiota studies of human disease. *Nature.* 2020;587(7834):448-454. https://doi.org/10.1038/s41586-020-2881-9

33. Krzyściak W, Pluskwa KK, Jurczak A, Kościelniak D. The pathogenicity of the *Streptococcus* genus. *Eur J Clin Microbiol Infect Dis.* 2013;32(11):1361-1376. https://doi.org/10.1007/s10096-013-1914-9

34. Dunn KA, MacDonald T, Rodrigues GJ, et al. Antibiotic and antifungal use in pediatric leukemia and lymphoma patients are associated with increasing opportunistic pathogens and decreasing bacteria responsible for activities that enhance colonic defense. *Front Cell Infect Microbiol.* 2022;12:924707. https://doi.org/10.3389/fcimb.2022.924707

35. Hou K, Wu ZX, Chen XY, et al. Microbiota in health and diseases. *Signal Transduct Targeted Ther.* 2022;7(1):135. https://doi.org/10.1038/s41392-022-00974-4

36. Manor O, Dai CL, Kornilov SA, et al. Health and disease markers correlate with gut microbiome composition across thousands of people. *Nat Commun.* 2020;11(1):5206. https://doi.org/10.1038/s41467-020-18871-1

37. Deleu S, Machiels K, Raes J, Verbeke K, Vermeire S. Short chain fatty acids and its producing organisms: an overlooked therapy for IBD? *EBioMedicine.* 2021;66:103293. https://doi.org/10.1016/j.ebiom.2021.103293

38. Koh A, De Vadder F, Kovatcheva-Datchary P, Bäckhed F. From dietary fiber to host physiology: short-chain fatty acids as key bacterial metabolites. *Cell.* 2016;165(6):1332-1345. https://doi.org/10.1016/j.cell.2016.05.041

39. Luu M, Riester Z, Baldrich A, et al. Microbial short-chain fatty acids modulate CD8^{+} T cell responses and improve adoptive immunotherapy for cancer. *Nat Commun.* 2021;12(1):4077. https://doi.org/10.1038/s41467-021-24331-1

40. Li X, Zhang S, Guo G, Han J, Yu J. Gut microbiome in modulating immune checkpoint inhibitors. *EBioMedicine.* 2022;82:104163. https://doi.org/10.1016/j.ebiom.2022.104163

41. McCulloch JA, Davar D, Rodrigues RR, et al. Intestinal microbiota signatures of clinical response and immune-related adverse events in melanoma patients treated with anti-PD-1. *Nat Med.* 2022;28(3):545-556. https://doi.org/10.1038/s41591-022-01698-2

42. Yamamoto ML, Schiestl RH. Intestinal microbiome and lymphoma development. *Cancer J.* 2014;20(3):190-194. https://doi.org/10.1097/ppo.0000000000000047

43. Yoon SE, Kang W, Chalita M, Lim J, Kim WS, Kim SJ. Comprehensive understanding of gut microbiota in treatment naïve diffuse large B cell lymphoma patients. *Blood.* 2021;138(suppl 1):2409. https://doi.org/10.1182/blood-2021-149881

44. Costabile A, Corona G, Sarnsamak K, et al. Wholegrain fermentation affects gut microbiota composition, phenolic acid metabolism and pancreatic beta cell function in a rodent model of type 2 diabetes. *Front Microbiol.* 2022;13:1004679. https://doi.org/10.3389/fmicb.2022.1004679

45. Mauro CSI, Hassani MK, Barone M, et al. Cerrado and Pantanal fruit flours affect gut microbiota composition in healthy and post-COVID-19 individuals: an in vitro pilot fermentation study. *Int J Food Sci Technol.* 2023;58(8):4495-4510. https://doi.org/10.1111/ijfs.16274

46. Zhao C, Dong H, Zhang Y, Li Y. Discovery of potential genes contributing to the biosynthesis of short-chain fatty acids and lactate in gut microbiota from systematic investigation in *E. coli. NPJ Biofilms Microbiomes.* 2019;5(1):19. https://doi.org/10.1038/s41522-019-0092-7

47. Kurita K, Ohta H, Shirakawa I, et al. Macrophages rely on extracellular serine to suppress aberrant cytokine production. *Sci Rep.* 2021;11(1):11137. https://doi.org/10.1038/s41598-021-90086-w

48. Agrawal S, Agrawal A, Said HM. Biotin deficiency enhances the inflammatory response of human dendritic cells. *Am J Physiol Cell Physiol.* 2016;311(3):C386-C391. https://doi.org/10.1152/ajpcell.00141.2016

49. Hughes ER, Winter MG, Duerkop BA, et al. Microbial respiration and formate oxidation as metabolic signatures of inflammation-associated dysbiosis. *Cell Host Microbe.* 2017;21(2):208-219. https://doi.org/10.1016/j.chom.2017.01.005

SUPPORTING INFORMATION

Additional supporting information can be found online in the Supporting Information section at the end of this article.